Electronic Supplementary Information for Dalton Transactions

An Unusual Discontinuity in the Thermal Spin Transition in $[Co(terpy)_2][BF_4]_2$

Colin A. Kilner and Malcolm A. Halcrow*

School of Chemistry, University of Leeds, Woodhouse Lane, Leeds, UK LS2 9JT.
E-mail: m.a.halcrow@leeds.ac.uk

Electronic Supplementary Information

Table S1 Selected bond lengths and angles in the crystal structures of $[Co(terpy)_2][BF_4]_2$ (Å, °). See Figure S1, and Figures 2 and 3 of the main paper, for the atom numbering scheme and for plots of these data.

T (K)	30	100	150	200	250	300	325	350	375
Co(1)–N(2)	1.907(3)	1.906(3)	1.938(2)	1.973(3)	2.013(3)	2.013(5)	2.041(4)	2.040(4)	2.045(4)
Co(1)–N(9)	2.066(2)	2.088(2)	2.0975(15)	2.1174(18)	2.135(2)	2.151(3)	2.149(2)	2.161(2)	2.160(3)
Co(1)–N(15)	2.066(2)	2.084(2)	2.0943(17)	2.109(2)	2.130(3)	2.147(3)	2.144(3)	2.158(3)	2.151(3)
Co(1)–N(20)	1.925(2)	1.912(2)	1.945(2)	1.976(3)	2.008(3)	2.003(4)	2.025(4)	2.033(4)	2.030(4)
Co(1)–N(27)	2.107(2)	2.088(2)	2.1023(17)	2.1165(19)	2.128(2)	2.141(3)	2.145(2)	2.150(2)	2.149(3)
Co(1)–N(33)	2.132(2)	2.107(2)	2.1193(16)	2.1313(19)	2.138(2)	2.153(3)	2.149(2)	2.155(2)	2.156(3)
N(2)–Co(1)–N(9)	80.19(9)	79.95(10)	79.17(7)	78.16(9)	77.36(11)	77.11(14)	76.88(12)	76.86(12)	76.78(14)
N(2)–Co(1)–N(15)	80.19(10)	79.44(10)	79.49(8)	78.77(10)	77.73(12)	77.21(15)	77.07(13)	76.68(13)	76.39(15)
N(2)–Co(1)–N(20)	178.22(12)	178.35(12)	178.18(9)	177.75(11)	178.08(13)	178.38(16)	178.20(13)	178.21(12)	178.36(12)
N(2)–Co(1)–N(27)	99.85(9)	99.87(9)	101.06(7)	102.57(8)	103.67(10)	104.29(12)	104.34(11)	104.48(10)	104.70(12)
N(2)–Co(1)–N(33)	101.48(9)	101.03(9)	101.20(7)	101.44(8)	101.94(10)	102.30(13)	102.52(11)	102.30(10)	102.28(12)
N(9)–Co(1)–N(15)	160.37(9)	159.39(9)	158.65(7)	156.91(9)	155.07(10)	154.30(13)	153.93(11)	153.53(11)	153.16(13)
N(9)–Co(1)–N(20)	98.11(9)	98.47(9)	99.01(7)	99.72(8)	100.87(10)	101.45(13)	101.63(11)	101.85(11)	102.35(13)
N(9)–Co(1)–N(27)	92.27(9)	92.31(8)	92.55(6)	92.92(7)	93.23(8)	93.55(11)	93.76(9)	93.68(9)	93.78(10)
N(9)–Co(1)–N(33)	93.91(9)	93.83(8)	93.88(6)	94.19(7)	94.47(8)	94.24(11)	94.26(9)	94.21(9)	94.30(10)
N(15)–Co(1)–N(20)	101.51(9)	102.13(9)	102.33(7)	103.37(9)	104.05(11)	104.25(14)	104.44(12)	104.62(12)	104.49(14)
N(15)–Co(1)–N(27)	90.55(9)	90.63(8)	90.79(6)	91.08(7)	91.59(9)	91.78(11)	91.85(9)	92.13(9)	92.16(10)
N(15)–Co(1)–N(33)	90.50(9)	90.67(8)	90.97(6)	91.34(7)	91.68(9)	92.15(11)	92.13(10)	92.14(10)	92.18(11)
N(20)–Co(1)–N(27)	79.63(9)	79.65(9)	78.99(7)	78.20(8)	77.10(10)	76.46(12)	76.69(11)	76.78(11)	76.70(12)
N(20)–Co(1)–N(33)	79.13(9)	79.53(9)	78.84(7)	77.90(9)	77.37(10)	77.01(12)	76.52(11)	76.49(11)	76.35(12)
N(27)–Co(1)–N(33)	158.51(9)	158.94(9)	157.62(7)	155.88(8)	154.29(10)	153.34(12)	153.07(11)	153.15(10)	152.94(12)
Σ[a]	89.0(3)	90.4(3)	95.3(3)	103.6(3)	111.9(3)	116.2(4)	117.8(4)	118.6(4)	120.0(4)
Θ[a]	300	305	318	341	364	378	380	383	387

[a] See the main text for the definitions of Σ and Θ, which are measures of the degree of angular distortion of the coordination sphere from an ideal octahedral geometry.

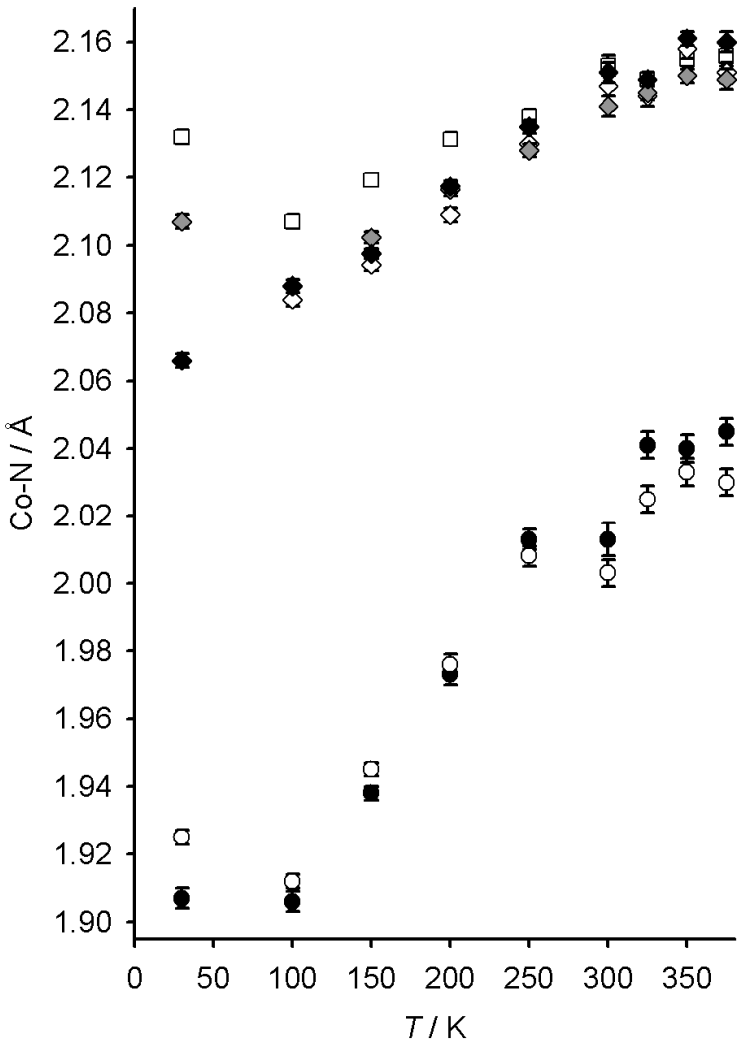

Fig. S1 Temperature dependence of the bond lengths in $[Co(terpy)_2][BF_4]_2$: Co(1)−N(2) (●); Co(1)−N(9) (◆); Co(1)−N(15) (◇); Co(1)−N(20) (○); Co(1)−N(27) (◈) and Co(1)−N(33) (□).

The increase in Co(1)−N(20), Co(1)−N(27) and Co(1)−N(33) on cooling from 100 to 30 K reflects freezing out of dynamic disorder, involving the axis Jahn-Teller elongation in the low-spin cobalt(II) centre. See ref. 15 of the main paper.

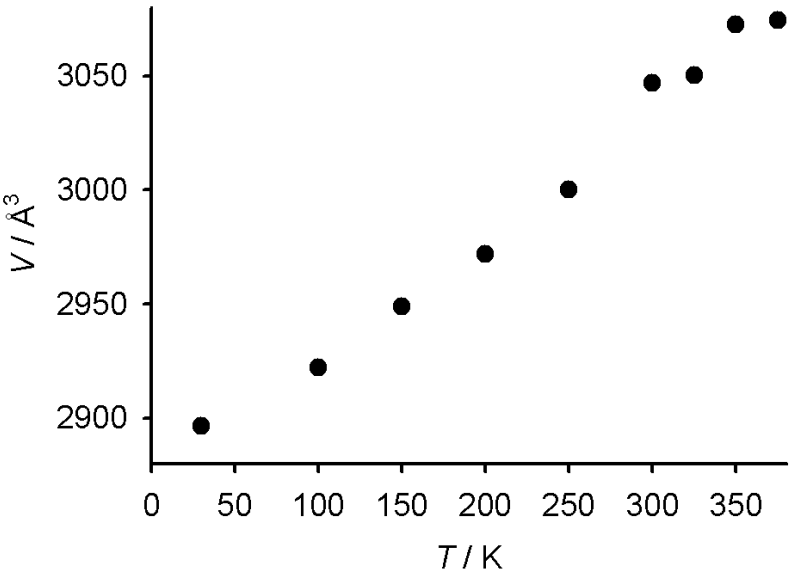

Fig. S2 Temperature dependence of the unit cell volume of $[Co(terpy)_2][BF_4]_2$. The temperature dependence of the individual unit cell parameters is shown in Fig. 3 of the main paper.

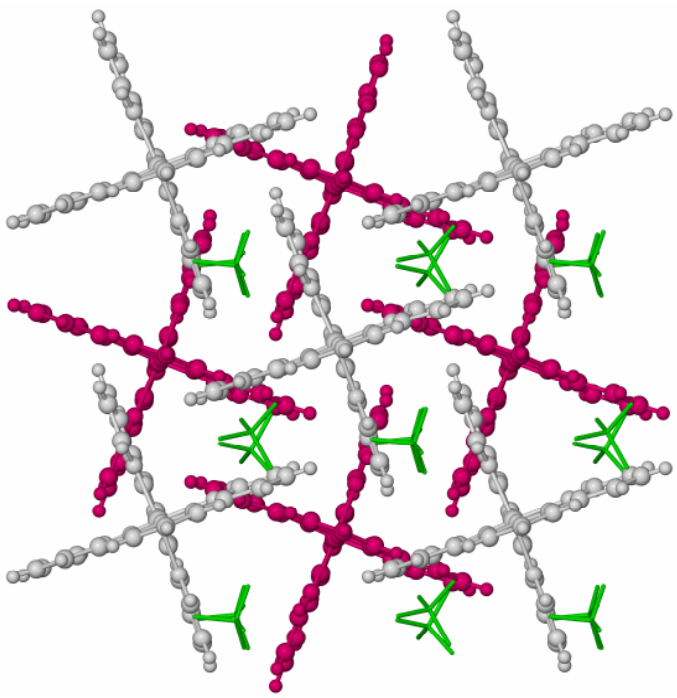

Fig. S3 Partial packing diagram of $[Co(terpy)_2][BF_4]_2$ at 300 K, showing the "terpyridine embrace" lattice.

The view is perpendicular to the [001] crystallographic vector, with [100] running horizontally. The complex dications associate into alternating four-fold layers, coloured white and pink. Only one orientation of the disordered BF_4^- ions is shown, which are de-emphasised and coloured green.

Table S2 Metric parameters for the unique intermolecular $\pi...\pi$ interactions in $[Co(terpy)_2][BF_4]_2$ (Å, °).

	[C(8)–C(13)]…[C(14^{i})–C(19^{i})]			[C(26)–C(31)]…[C(32^{ii})–C(37^{ii})]		
Colour in Fig. S4	Black			Green		
T (K)	Distance	Angle	Offset	Distance	Angle	Offset
30[a]	3.586(9)	8.74(9)	1.36	3.407(9)	8.69(11)	1.55
100[b]	3.581(9)	8.46(10)	1.37	3.431(9)	7.81(11)	1.55
150[a]	3.571(7)	7.74(7)	1.36	3.451(7)	7.39(9)	1.50
200[a]	3.567(9)	7.19(9)	1.32	3.472(9)	6.71(11)	1.45
250[a]	3.567(11)	6.65(11)	1.29	3.488(11)	6.43(13)	1.42
300[b]	3.582(14)	6.13(15)	1.31	3.516(15)	6.28(18)	1.45
325[a]	3.584(13)	6.00(13)	1.30	3.525(13)	5.98(15)	1.39
350[a]	3.595(13)	5.82(14)	1.30	3.536(13)	5.73(15)	1.40
375[a]	3.596(15)	5.76(16)	1.31	3.538(14)	5.57(17)	1.39

[a]Symmetry codes: (i) ½+*x*, ½+*y*, *z*; (ii) ½+*x*, ½−*y*, *z*. [b]Symmetry codes: (i) ½−*x*, ½−*y*, *z*; (ii) ½−*x*, ½+*y*, *z*.

Table S3 Metric parameters for the unique intermolecular C−H -π interactions in $[Co(terpy)_2][BF_4]_2$ (Å, °). The H...π distances and C–H...π angles are calculated to the centroid of the acceptor pyridine ring. The colours listed refer to the points in the corresponding graphs in Fig. S4.

	C(11)–H(11)…[C(26^{i})–C(31^{i})]		C(18)–H(18)…[C(32^{iii})–C(37^{iii})] {C(17)−H(17)…[C(32^{iii})–C(37^{iii})]}[c]		C(29)–H(29)…[C(14^{ii})–C(19^{ii})]		C(35)–H(35)…[C(7^{iv})–C(13^{iv})]	
Colour	Red		Grey		Yellow		Cyan	
T (K)	Distance	Angle	Distance	Angle	Distance	Angle	Distance	Angle
30[a]	3.07	152.9	2.96 {3.23}	134.2 {120.1}	2.96	134.5	2.86	141.0
100[b]	3.08	153.4	2.98 {3.23}	133.5 {121.8}	2.98	134.8	2.89	140.6
150[a]	3.12	154.2	3.02 {3.22}	132.5 {123.2}	2.99	137.3	2.91	141.7
200[a]	3.12	155.3	3.10 {3.15}	129.3 {126.4}	2.98	140.3	2.93	142.7
250[a]	3.12	155.7	3.21 {3.09}	125.2 {130.0}	2.98	143.0	2.94	143.8
300[b]	3.14	156.2	3.29 {3.08}	123.7 {132.0}	3.01	143.5	2.96	145.1
325[a]	3.14	156.5	3.28 {3.07}	124.1 {133.1}	3.01	144.7	2.97	144.8
350[a]	3.16	156.4	3.33 {3.08}	122.9 {133.7}	3.03	144.7	2.99	144.9
375[a]	3.16	156.7	3.35 {3.09}	122.5 {134.4}	3.03	144.9	2.99	145.4

[a]Symmetry codes: (i) ½+*x*, ½+*y*, *z*; (ii) ½+*x*, ½−*y*, *z*; (iii) ½−*x*, ½−*y*, *z*; (iv) ½−*x*, ½+*y*, *z*. [b]Symmetry codes: (i) ½−*x*, ½−*y*, *z*; (ii) ½−*x*, ½+*y*, *z*; (iii) ½+*x*, ½+*y*, *z*; (iv) ½+*x*, ½+*y*, *z*. [c]The shortest distance between these two pyridyl groups changes as the temperature is raised (Fig. 5 of the main paper).

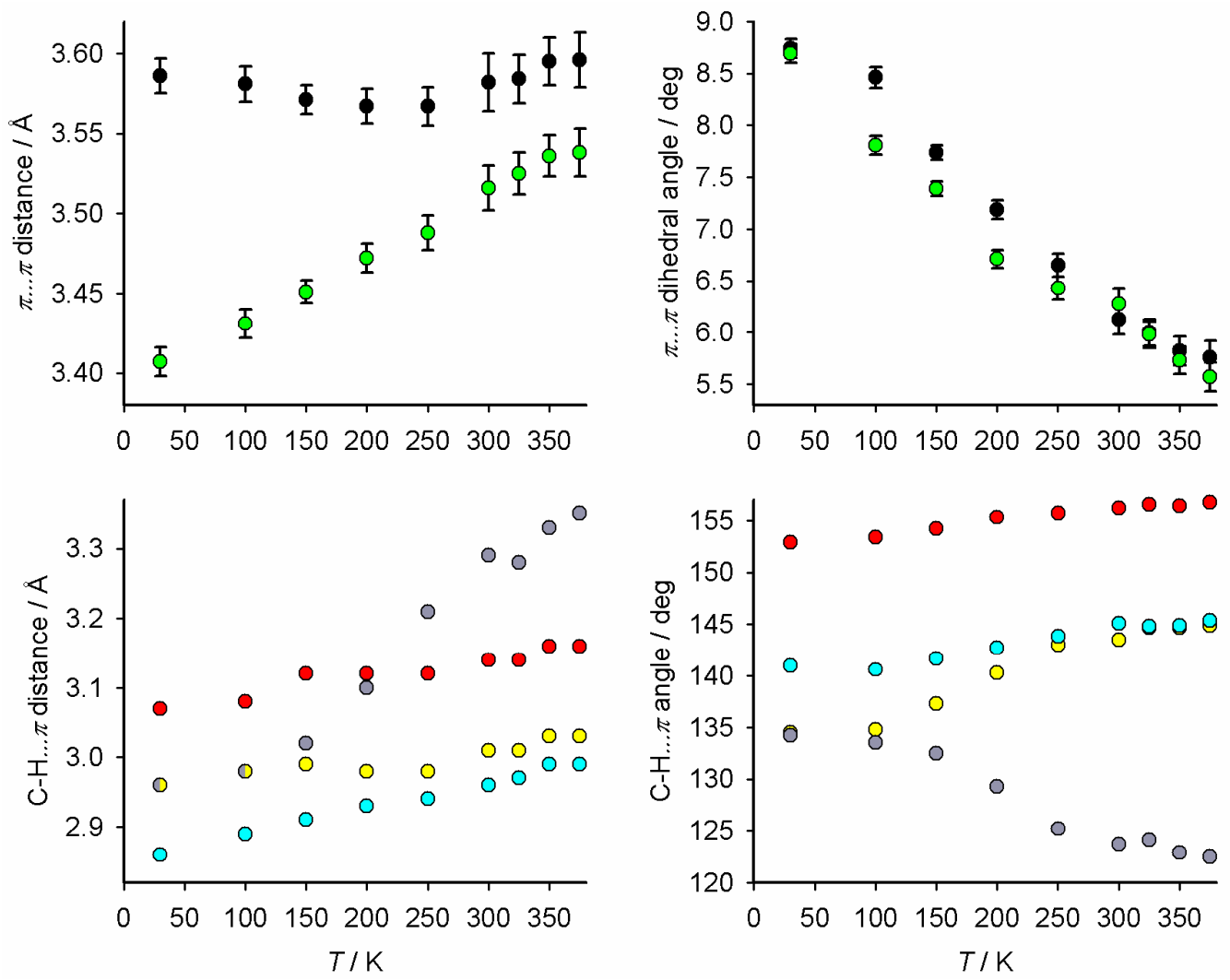

Fig. S4 Plots of the temperature dependence of the metric parameters for the intra-layer intermolecular interactions in $[Co(terpy)_2][BF_4]_2$. The data, and the colour codes for the different datapoints, are listed in Tables S2 and S3.

There is no unusual temperature-dependent variation in the geometry of the $\pi...\pi$ interactions, within experimental error. However, there are some apparent irregularities in the temperature dependence of the C–H...π contacts, particularly for C(18)–H(18)…[C(32^{iii})–C(37^{iii})] (the grey points in the Figure; Table S3). It is unclear whether these are statistically significant, though.

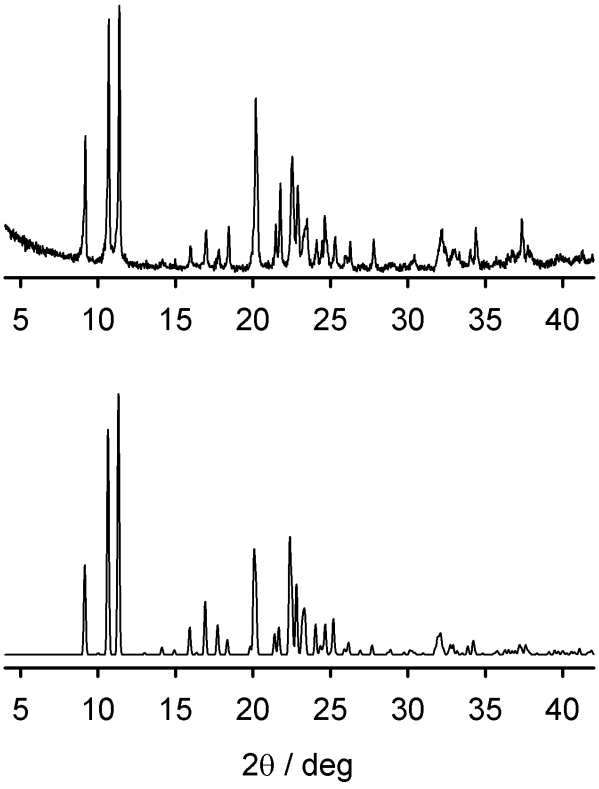

Fig. S5 Observed (top) and simulated (bottom) *X*-ray powder diffraction data for $[Co(terpy)_2][BF_4]_2$ at 298 K (λ = 1.5418 Å).

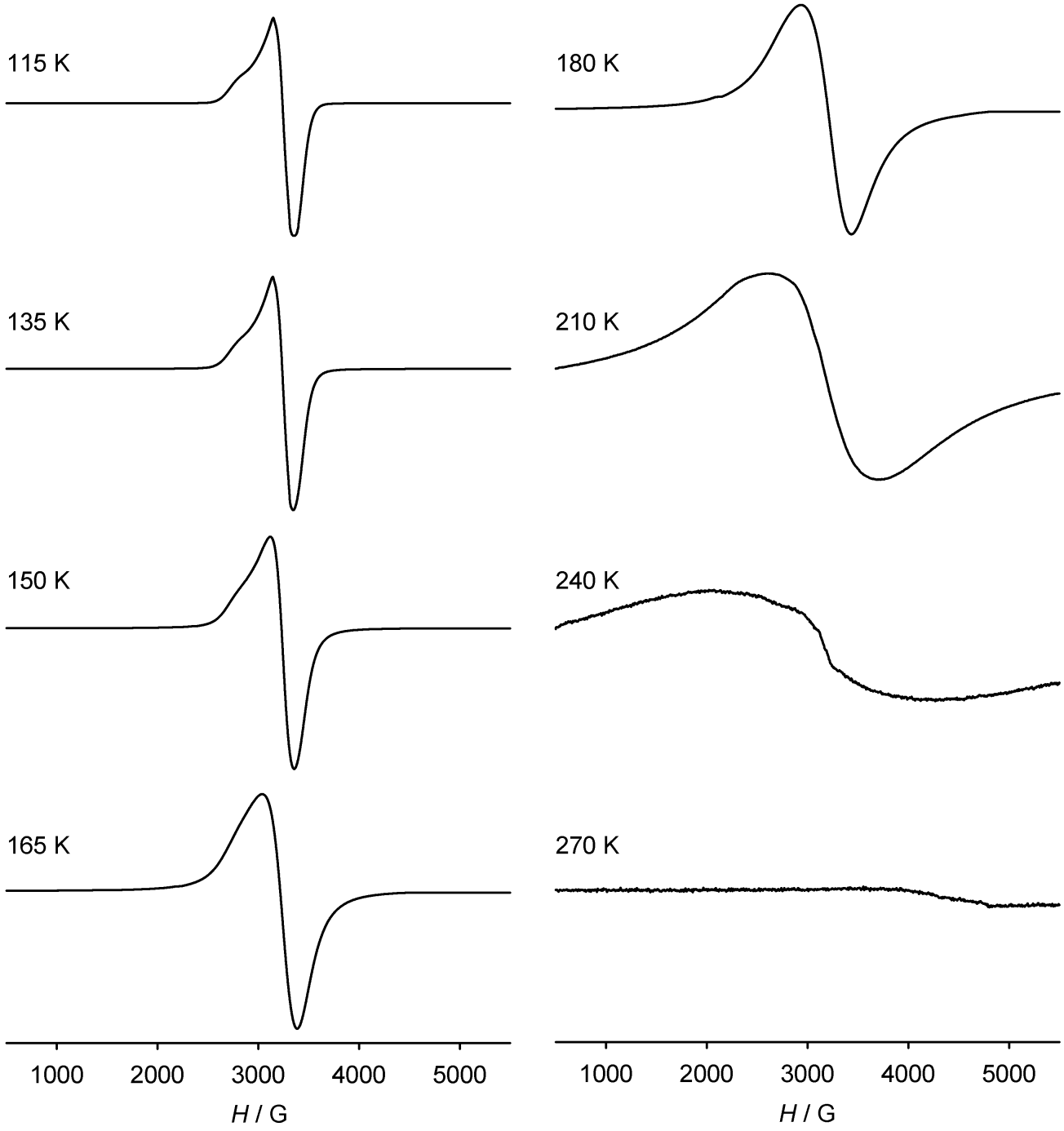

Fig. S6 Variable temperature *X*-band powder EPR spectra of $[Co(terpy)_2][BF_4]_2$ (ν = 9.54 GHz).

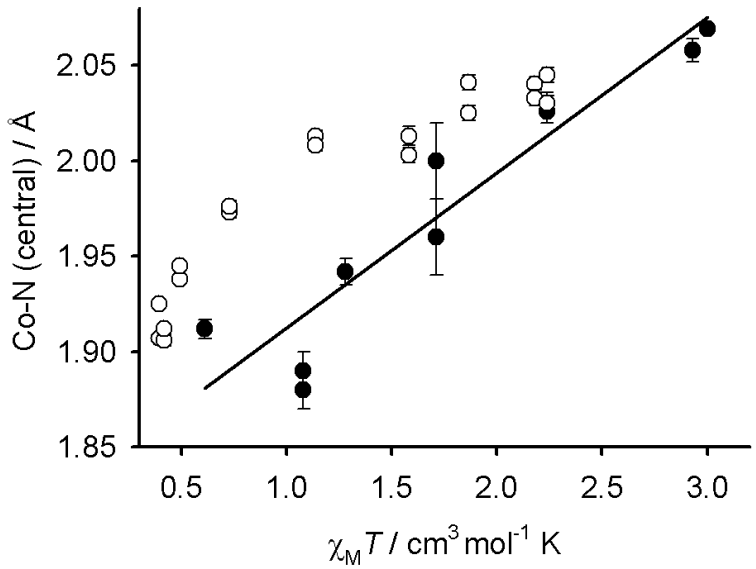

Fig. S7 Plot of central Co−N bond lengths (Co(1)−N(2) and Co(1)−N(20) in $[Co(terpy)_2][BF_4]_2$) *vs.* $\chi_M T$ from powder susceptibility measurements in $[Co(terpy)_2][BF_4]_2$ (○) and other $[Co(terpy)_2]^{2+}$ salts (●).[1] The line corresponds to the magnetostructural correlation proposed in ref. [1].Only literature compounds where crystallographic and magnetic data are available at the same temperature are included.[2]

The fact that the points for $[Co(terpy)_2][BF_4]_2$ lie above the proposed correlation line may reflect the apparently lower temperature of the spin-transition in the crystal compared to powder samples of the material.

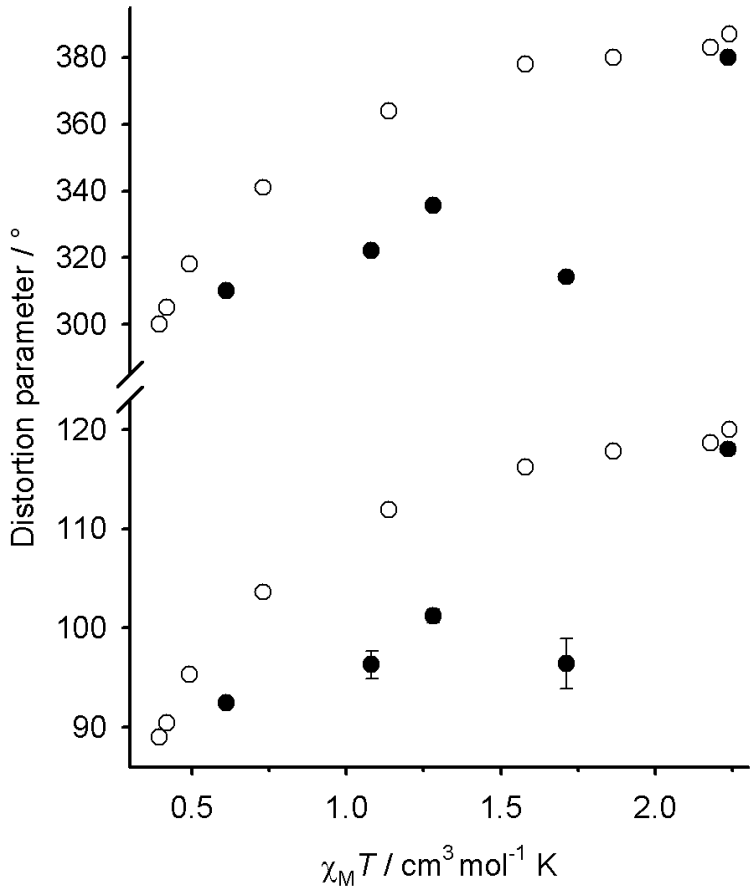

Fig. S8 Plot of crystallographic Σ (bottom) and Θ (top) values *vs.* $\chi_M T$ from powder susceptibility measurements in $[Co(terpy)_2][BF_4]_2$ (○) and other $[Co(terpy)_2]^{2+}$ salts (●).[1,2] See the main text for the definitions of Σ and Θ.

Notes and references

[1] B. N. Figgis, E. S. Kucharski and A. H. White, *Aust. J. Chem.*, 1983, **36**, 1537.

[2] Only one $[Co(terpy)_2]^{2+}$ salt has been crystallographically characterised in a known spin-state since ref. [1] was published. That is $[Co(terpy)_2][Mn(H_2O)Cr(ox)_3]_2{\cdot}5H_2O{\cdot}½MeOH$, which has been described as "low-spin" on the basis of its magnetic behaviour, although it is difficult to deconvolute the individual contributions of the Co, Mn and Cr centres to the magnetic moment of the compound.[3] We have not included it in Figs. S7 and S8, because we believe its crystal structure has been mis-assigned as a cobalt(II) complex and is actually a salt of $[Co(terpy)_2]^{3+}$. Its Co−N bond lengths are unusually short for a cobalt(II) terpy complex, but closely resemble those of $[Co(terpy)_2]Cl_3$.[4] Moreover, a bond-valence sum (BVS) calculation[5,6] gives a BVS of 3.05 for $[Co(terpy)_2][Mn(H_2O)Cr(ox)_3]_2{\cdot}5H_2O{\cdot}½MeOH$. For comparison the BVS is 3.11 for $[Co(terpy)_2]Cl_3$;[4] 2.32 for the related cobalt(II) material $[Co(terpy)_2][Mn(H_2O)ClCr(ox)_3]{\cdot}H_2O{\cdot}½MeOH$;[3] and, 1.78-2.27 for $[Co(terpy)_2][BF_4]_2$ at different temperatures.

[3] H.-Z. Kou and O. Sato, *Inorg. Chem.*, 2007, **46**, 9513.

[4] B. N. Figgis, E. S. Kucharski and A. H. White, *Aust. J. Chem.*, 1983, **36**, 1563.

[5] M. O'Keeffe and N. E. Brese, *J. Am. Chem. Soc.*, 1991, **113**, 3226.

[6] R. M. Wood and G. J. Palenik, *Inorg. Chem.*, 1998, **37**, 4149.